IOP Publishing | Society for Radiological Protection Journal of Radiological Protection
J. Radiol. Prot. **39** (2019) 838–853 (16pp) https://doi.org/10.1088/1361-6498/ab29a3

Assessment of long-term risks of secondary cancer in paediatric patients with brain tumours after boron neutron capture therapy

Xinxin Zhang[1], Changran Geng[1], Xiaobin Tang[1,4], Silva Bortolussi[2,3], Diyun Shu[1], Chunhui Gong[1,2], Yang Han[1] and Shaojuan Wu[1]

[1] Department of Nuclear Science and Technology, Nanjing University of Aeronautics and Astronautics, Nanjing 210016, People's Republic of China
[2] Unit of Pavia, National Institute of Nuclear Physics (INFN), Pavia 27100, Italy
[3] Department of Physics, University of Pavia, Pavia 27100, Italy

E-mail: tangxiaobin@nuaa.edu.cn

Received 15 April 2019, revised 10 June 2019
Accepted for publication 13 June 2019
Published 7 August 2019

Abstract

This study firstly explored the risks of secondary cancer in healthy organs of Chinese paediatric patients with brain tumours after boron neutron capture therapy (BNCT). Three neutron beam irradiation geometries (i.e. right lateral, top to bottom, posterior to anterior) were adopted in treating patients with brain tumours under the clinical environment of BNCT. The concerned organs in this study were those with high cancer morbidity in China (e.g. lung, liver and stomach). The equivalent doses for these organs were calculated using Monte Carlo and anthropomorphic paediatric phantoms with Chinese physiological features. The risk of secondary cancer, characterised by the lifetime attributable risk (LAR) factor given in the BEIR VII report, was compared among the three irradiation geometries. The results showed that the LAR was lower with the PA irradiation geometry than with the two other irradiation geometries when the 2 cm diameter tumour was at a depth of 6 cm on the right side of the brain. Under the PA irradiation geometry, the LAR in the organs increased with increasing tumour volume and depth because of the long irradiation time. As the patients aged from 10–15 years old, the LAR decreased, which was related to the increased patient height and shortened life expectancy. Female patients had a relatively higher risk of secondary cancer than male patients in this study, which could be due to the thinner body

[4] Author to whom any correspondence should be addressed.

thickness and the weaker protective effect on the internal organs of the female patients. In conclusion, the risks of secondary cancer in organs were related to irradiation geometries, gender, and age, indicating that the risk of secondary cancer is a personalised parameter that needs to be evaluated before administering BNCT, especially in patients with large or deep tumours.

Keywords: radiation-induced second cancer risk, BNCT, Monte Carlo simulation, equivalent dose

(Some figures may appear in colour only in the online journal)

1. Introduction

Boron neutron capture therapy (BNCT) is based on the nuclear capture and fission reactions that occur when boron-10, a non-radioactive constituent of boron, is irradiated with a thermal or epithermal neutron beam [1]. BNCT has become an innovative technology in radiation therapy because of its targeted treatment, low toxicity, and high efficiency. Since the last century, BNCT has emerged in various countries, such as Japan, Finland, Italy, and China [2]. Given its strong biological effects, BNCT has unique advantages in the treatment of head and neck tumours [3], glioma, and melanomas. Nowadays, accelerator-based neutron sources are being focused on and are developing rapidly. Accelerator-based boron capture therapy (AB-BNCT) facilities are being constructed worldwide [4], to start an era of in-hospital facilities [5].

Aside from the dose delivered to the target organ in a BNCT treatment, the scattering neutron and the induced high-energy gamma rays [6] in the human body could deposit doses in healthy organs, which may induce the risk of secondary cancer. As early as the 1940s, Cahan *et al* defined the criteria for classifying radiation-induced secondary cancer [7]. The risk of secondary cancer is the probability of a tumour occurring in a healthy organ irradiated by primary or secondary therapeutic beams outside the target area with a latency period of several years [7]. The risk of radiation-induced cancer and late tissue injury is receiving increasing attention, and radiation-induced secondary cancer in cancer survivors cannot be ignored, especially in children with long life expectancies. Several dosimetry studies were performed to evaluate the risk of secondary cancer in healthy organs of patients treated with photons, protons, and heavy ions [8–10]. The incidence of the risk of secondary cancer in healthy organs has been related to many factors, and long-term survivors of childhood cancer who receive radiotherapy have a considerably high risk of developing secondary cancer. Thus, secondary cancer should be explored to understand and prevent late-occurring effects in paediatric tumour survivors while preserving the high rates of local control and long-term survival [11].

However, at present, no studies have concentrated on the risk of secondary cancer of BNCT treatments, during which neutrons, gamma, and heavy ions are all involved. In consideration of the increased future application of BNCT in patients with cancer, its risk of secondary cancer needs to be evaluated to provide radiation protection to patients, especially children. Given its high tumour selectivity and high biological effectiveness, BNCT has unique advantages in the treatment of brain tumours, which are common in childhood [12]. The research on the risk of secondary cancer in paediatric patients treated with BNCT has important clinical significance. Therefore, this study aimed to assess the risk of secondary cancer in the healthy organs of Chinese paediatric patients with brain tumours after BNCT;

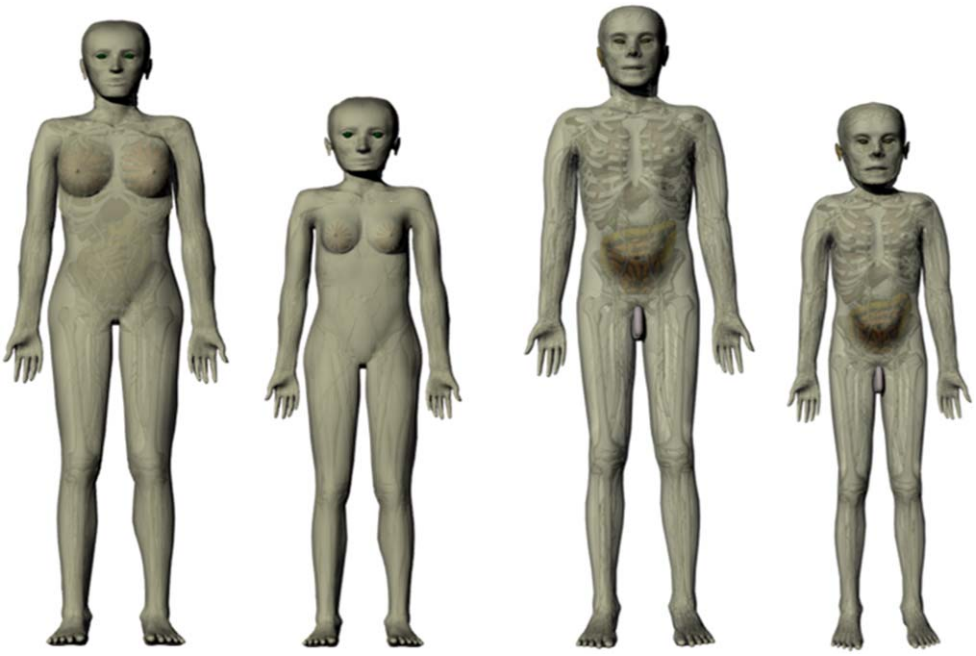

Figure 1. Chinese hybrid radiation phantoms, from left to right: 15-year-old female, 10-year-old female, 15-year-old male, 10-year-old male.

preliminarily explore the effects of irradiation geometry, tumour volume, and depth, and patient gender and age on the risk of secondary cancer.

2. Methods

2.1. Radiation computational phantom

In this study, Chinese hybrid radiation female and male phantoms of 10 and 15 years old were adopted, as shown in figure 1. They were created by our research group at the Nanjing University of Aeronautics and Astronautics [13] with particular Chinese physiological features. The original anatomy of the phantom was obtained from Anatonium^{TM} 3D P1 V5.0, including almost all organs, skeleton, blood vessels, and lymph of the human body [13]. The number of organs and tissues were 49 and 47 for the female and male phantoms, respectively. This study focused on brain tumours 2 cm in diameter and 6 cm in depth on the right side of the head, as shown in figure 2.

2.2. Irradiation configuration

According to the treatment methods commonly used in BNCT, three irradiation geometries were studied (i.e. right lateral (RLAT), top to bottom (TOP) and posterior to anterior (PA)), as shown in figure 2. For each irradiation geometry, the airgap between the neutron source and the patient surface is 10 cm. The center of the tumour corresponds to the center of the incident source in this study, ensuring that the tumour is all within the field. The diffusion angle is set in the Monte Carlo simulation to represent the scattering and leakage of the incident neutron

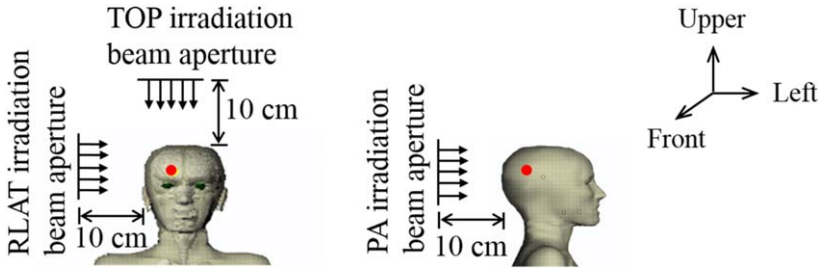

Figure 2. Brain tumour location (the red circle) and three irradiation geometries.

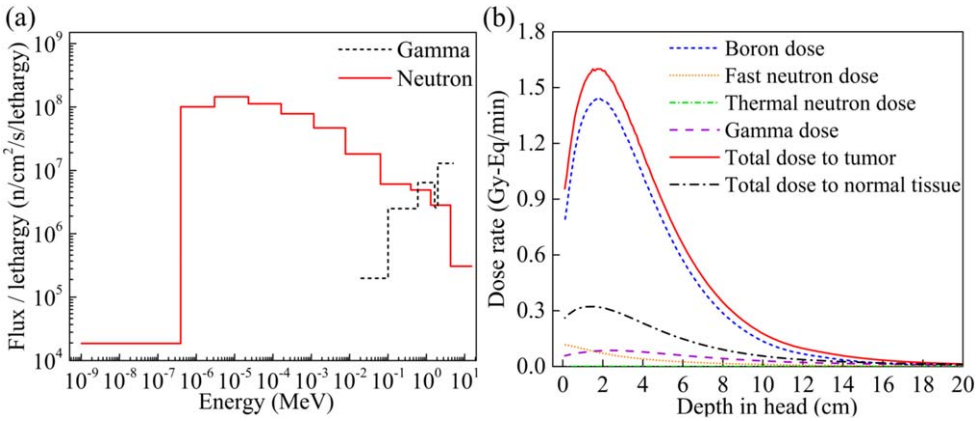

Figure 3. (a) Energy spectrum of the beam source; (b) curve of the depth dose in the head phantom for normal tissue and the tumour.

source. The incident neutron and photon source energy spectrum [14, 15] are shown in figure 3(a). The radius of the beam aperture is 5 cm, and the curve of the dose depth obtained from the irradiation of the head is shown in figure 3(b). In accordance with the clinical treatment of brain tumours, the prescribed dose for brain tumours is 20 Gy-Eq for the three irradiation geometries [16], which can effectively kill tumours.

2.3. Risk of secondary cancer calculation model

The risk model given in the BEIR VII report [17] was used to evaluate the risk of secondary cancer induced by BNCT. The establishment of this risk model was based on data from the Japanese atomic bomb survivors. The model considers parameters such as gender, organ, and age of exposure. The excess relative risk (ERR) and excess absolute risk (EAR) model recommended in the BEIR VII report can be obtained by

$$\text{ERR and EAR} = \beta_s D \exp(\gamma e^*)\left(\frac{a}{60}\right)^{\eta} \tag{1}$$

where D is the radiation dose to the organ; β_S, γ, and η are the ERR- and EAR-specific parameters for various organs for each sex; e is the age at exposure; $e^* = (e\text{-}30)/10$ for $e < 30$ and 0 for $e > 30$ years; and a is the attained age. The form of the model for leukaemia is different from the ERR and EAR above. Readers can refer to the BEIR VII report [17] for

organs other than the oesophagus and brain, and the β_S for the oesophagus and brain is based on the study by Berrington de Gonzalez *et al* [18].

The risk of secondary cancer of organs other than the breast, lung, and thyroid was assessed on the basis of the lifetime attributable risk (LAR) [19] recommended in the BEIR VII report, as given in equation (2).

$$\mathrm{LAR}_{(D,e)} = \left(\sum_{e+L}^{100} \mathrm{ERR}(D,\, e,\, a) \times \lambda_I^C \times \frac{S(a)}{S(e)}\right)^{0.7} \times \left(\sum_{e+L}^{100} \mathrm{EAR}(D,\, e,\, a) \times \frac{S(a)}{S(e)}\right)^{0.3} / \mathrm{DDREF}. \tag{2}$$

ERR (D, e, a) and EAR (D, e, a) are described in equation (1), and λ_I^C represents the baseline cancer risk and is based on the statistics for the Chinese population. $S(a)/S(e)$ is the probability of surviving to the attained age (a) conditional on survival to exposed age (e) and is derived from the life span tables of the Sixth National Census in China. The latency period (L) is 5 years for solid cancer and 2 years for leukaemia. The dose and dose-rate effectiveness factor (DDREF) is applied for all cancer sites except leukaemia when the dose of organs is within 100 mGy and is 1.5 in the calculation of LARs as recommended in the BEIR VII report [17] and Berrington de Gonzalez *et al* [18]. The weights 0.7 and 0.3 in equation (2) are recommended by the BEIR Committee for most organs. The weights of 0.7 and 0.3 are reversed for the lung, only the EAR model is recommended for the breast, and the LAR is calculated using the ERR model only for the thyroid [19].

2.4. Monte Carlo simulation and dose calculation

The TOol for PArticle Simulation (TOPAS) Monte Carlo code [20] was used in the dose calculations for the brain tumour treatment by BNCT. TOPAS is a Monte Carlo platform based on Geant4. It not only retains all the features of Geant4 in terms of speed, accuracy, and flexibility but also provides standardised basic physics. The physical model 'g4em-standard_opt4,' 'thermalphp physics,' 'g4decay,' 'g4ion-binarycascade,' 'g4h-elastic_HP,' 'g4stopping,' and 'g4em-extra' were adopted in this research as described in previous studies [21]. The number of simulated particles was 1×10^9, and the Monte Carlo uncertainty was less than 3%, ensuring the accuracy of the simulation results. The boron concentrations [22, 23] of the tumour, organs, and skin were 60, 18, and 25 ppm, respectively, in accordance with the research of boron drugs in BNCT [24, 25]. The phantom was voxelised, and the volume of each voxel was $5 \times 5 \times 5\,\mathrm{mm}^3$. The doses for the tumour and organs were calculated by the counting card combined with the kerma factor [26]. The doses for the tumour and organs were mainly divided into four parts: boron dose D_B, fast neutron dose D_f, thermal neutron dose D_th, and gamma dose D_γ. The boron dose is from the fission fragments of the reaction $^{10}\mathrm{B}(\mathrm{n}, \alpha)^7\mathrm{Li}$. The equivalent dose H was obtained by multiplying the doses of the different components and the corresponding relative biological effectiveness [27] or combined biological effect, as shown in equation (3).

$$H = W_\mathrm{B} \times D_\mathrm{B} + W_\mathrm{f} \times D_\mathrm{f} + W_\mathrm{th} \times D_\mathrm{th} + D_\gamma. \tag{3}$$

For the tumour, W_B, W_f, and W_th are respectively defined as 3.8, 3.2, and 3.2; for normal organs, W_B, W_f, and W_th are respectively defined as 1.4, 3.2, and 3.2; for the skin, W_B, W_f, and W_th are respectively defined as 2.5, 3.2, and 3.2 [28, 29].

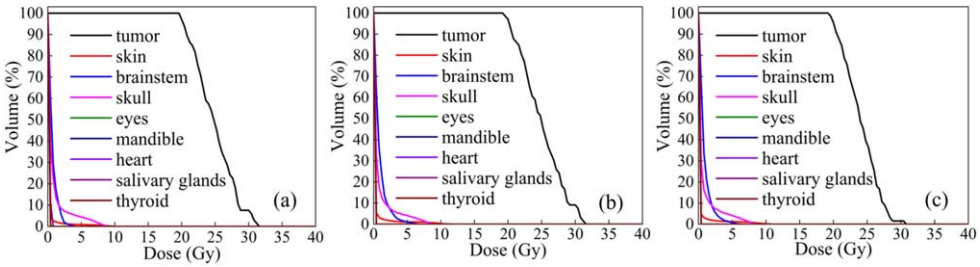

Figure 4. Dose volume histograms for tumour and organs in a 10-year-old female phantom for the (a) RLAT, (b) TOP and (c) PA irradiation geometries. (The figure may only appear in colour in the online journal.)

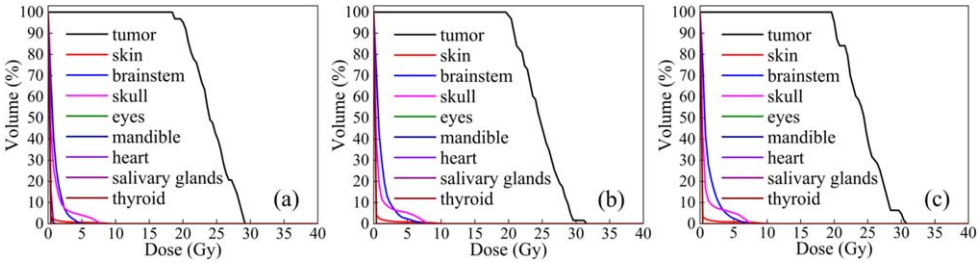

Figure 5. Dose volume histograms for tumour and organs in a 15-year-old female phantom for the (a) RLAT, (b) TOP, and (c) PA irradiation geometries. (The figure may only appear in colour in the online journal.)

3. Results

3.1. Effect of irradiation geometries on the risk of secondary cancer

The dose volume histograms of the tumour and organs at risk obtained from the three irradiation geometries of females aged 10 and 15 are shown in figures 4 and 5, respectively. On the premise that the dose to 95% of the tumour volume is 20 Gy-Eq in this study, the irradiation times are 30, 28.5, and 28.4 min with the RLAT, TOP, and PA irradiation geometries for the 10-year-old female patients and 28.9, 27.4, and 27.4 min for the 15-year-old female patients, respectively. The equivalent dose can be obtained by multiplying the physical dose with the corresponding relative biological effectiveness, and its unit is Gy-Eq. According to the recommended dose limits of National Comprehensive Cancer Network (NCCN) [30], the doses for the skin, brainstem, skull, eyes, mandible, heart, salivary gland, thyroid and other organs at risk of the 10 and 15-year-old female patients do not exceed the limit. The maximum skin doses are 12.13, 11.45 and 11.17 Gy-Eq for the 10-year-old female patients, and 11.52, 10.81 and 10.86 Gy-Eq for the 15-year-old patients under the three irradiation geometries, respectively.

In this study, the organs of concern are those with high cancer incidence in China. The organ equivalent doses of the 10- and 15-year-old female patients under the three irradiation geometries are shown in figure 6. The distance and tissue shielding presented between the incident source and specific organs mainly affects the equivalent dose of the healthy organs. In all three irradiation geometries, the equivalent dose of the brain is the highest in the organs of concern, and it is related to the positional relationship between the brain and the incident

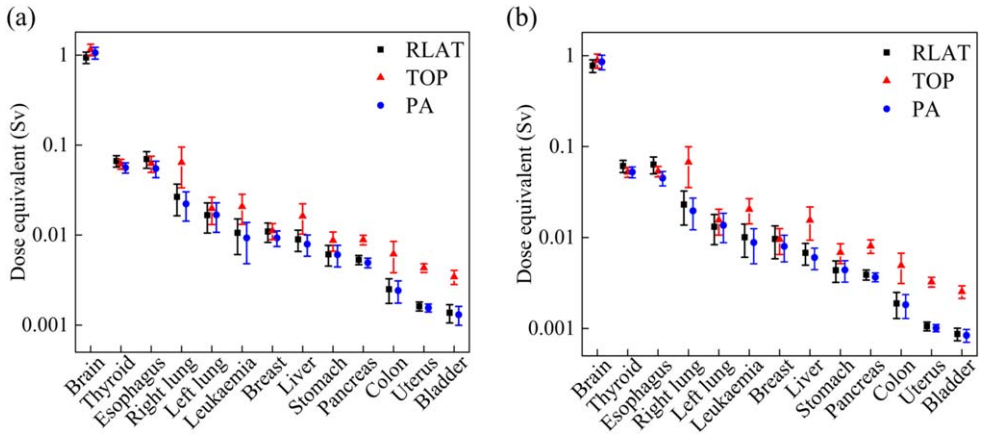

Figure 6. Organ equivalent dose under the three irradiation geometries. (a) 10-year-old female patients, (b) 15-year-old female patients. (The error bar is the standard deviation.)

source. The TOP irradiation geometry shows a slightly higher equivalent dose to the abdominal organs compared with the two other irradiation geometries, which is related to the different incident neutron beam paths. Among the three geometries, the PA geometry delivers the lowest doses overall. The effective dose of the 10-year-old female patients under the PA geometry is about 0.31 Sv, approximately equal to 31 CT scans if the dose received by a patient on a CT scan is assumed to be 10 mSv.

The risks of secondary cancer in organs under the three irradiation geometries are shown in table 1. The LARs are variable for the different organs. The LARs are higher in the brain, thyroid, oesophagus, lung, and breast than in other organs. The LAR in the brain is much higher than other organs of concern because of its high equivalent dose. The LARs in organs under the TOP irradiation geometry are significantly higher than those in organs under the two other irradiation geometries. Especially in the right lung, the LARs for the 10-year-old female patients are respectively 101, 244 and 84 per 100 000 population for the RLAT, TOP and PA irradiation geometries. The overall estimation of LAR indicates that the risk of radiation-induced cancer is lower with the PA irradiation geometry than with the RLAT or TOP irradiation geometry when the tumour under this simulated condition achieves the same therapeutic effect.

3.2. Effect of tumour volume on the risk of secondary cancer

Under the PA irradiation geometry, the effect of tumour volume on the risk of secondary cancer in healthy organs is investigated. Small, medium, and large tumours are those with 1, 2, and 5 cm diameters, respectively. The treatment times for the three tumour volumes are 25.5, 28.4 and 40.6 min, respectively, for the 10-year-old female patients, and 24.7, 27.8 and 39.2 min, respectively, for the 15-year-old female patients. The maximum doses to the skin for the three tumour volumes are 10.32, 11.12 and 16.38 Gy-Eq for the 10-year-old female patients, respectively, and 9.89, 10.86 and 15.68 Gy-Eq for the 15-year-old female patients, respectively. For patients aged 10 or 15 years old, the maximum doses of the organs at risk, such as the eyes, brainstem, and skull, are all within the dose limit recommended by NCCN [30].

Table 1. Lifetime attributable risks in organs and ages at exposure to three different irradiation geometries (per 100 000 population).

	Females (10 yr)			Females (15 yr)		
	RLAT (95% CI[a])	TOP (95% CI)	PA (95% CI)	RLAT (95% CI)	TOP (95% CI)	PA (95% CI)
Brain	355 (133, 696)	435 (163, 851)	400 (150, 784)	194 (73, 380)	221 (83, 433)	214 (80, 419)
Thyroid	154 (41, 573)	143 (38, 531)	130 (35, 483)	86 (23, 320)	74 (20, 274)	74 (20, 275)
Oesophagus	50 (<0, 201)	45 (<0, 179)	39 (<0, 157)	42 (<0, 167)	38 (<0, 152)	34 (<0, 136)
Right lung	101 (68, 147)	244 (164, 355)	84 (57, 123)	67 (45, 98)	196 (132, 286)	57 (39, 83)
Left lung	63 (43, 92)	75 (50, 109)	64 (43, 93)	38 (26, 56)	45 (31, 66)	40 (27, 58)
Breast	68 (48, 96)	69 (49, 98)	58 (41, 81)	59 (42, 83)	60 (43, 84)	49 (35, 70)
Liver	7 (2, 19)	12 (4, 35)	6 (2, 17)	4 (1, 10)	8 (3, 24)	3 (1, 9)
Stomach	13 (8, 19)	18 (12, 27)	12 (8, 19)	6 (4, 10)	10 (6, 15)	7 (4, 10)
Pancreas	4 (<0, 10)	7 (<0, 16)	4 (<0, 9)	2 (<0, 4)	4 (<0, 8)	2 (<0, 4)
Colon	4 (2, 8)	9 (4, 20)	4 (2, 8)	2 (1, 4)	5 (2, 11)	3 (1, 7)
Leukaemia	7 (1, 16)	13 (1, 31)	6 (1, 14)	5 (1, 10)	9 (1, 21)	4 (0, 9)
Bladder	1 (1, 3)	3 (1, 7)	1 (0, 3)	1 (0, 1)	2 (1, 4)	1 (0, 1)
Uterus	1 (<0, 1)	1 (<0, 3)	1 (<0, 2)	0 (<0, 1)	1 (<0, 1)	0 (<0, 1)

[a] CI represents the confidence intervals for LAR using the 95% range of β according to the BEIR VII report [17] and the study by Berrington de Gonzalez *et al* [18].

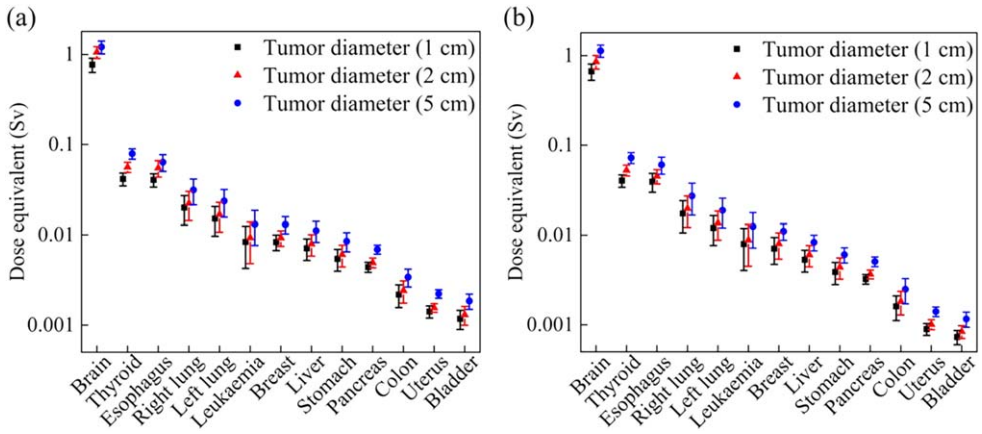

Figure 7. Organ equivalent dose for different tumour volumes: (a) female patients aged 10 years, (b) female patients aged 15 years. (The error bar is the standard deviation.)

The equivalent organ doses of the 10- and 15-year-old female patients are shown in figure 7. With the growth of the tumour volume, the exposure time of healthy organs is longer and the organs' equivalent doses become larger. With the exception of the brain, the thyroid has the highest equivalent dose, ranging from 40–80 mSv depending on the different tumour volumes for the 10-year-old female patients. The equivalent doses for the uterus and bladder are the lowest among the organs concerned.

Table 2 shows the risks of secondary cancer in healthy organs of female patients aged 10 and 15 years with different tumour volumes. In consideration that the risks of secondary cancer are proportional to the organ dose, the comparison of the different tumour volumes in terms of LAR yields the same findings as the comparison of the various tumour volumes in terms of equivalent dose. The LAR in the thyroid is much higher than that in the other organs. When the tumour diameters of the 10-year-old female patients are 1 and 5 cm, the LARs of secondary cancer in the thyroid are 96 and 183 per 100 000 population, respectively, and approximately increased twice. As the tumour diameters change from 1–5 cm, the irradiation time becomes longer, and the organ equivalent dose is generally increased linearly, and the risks of secondary cancer in most organs increased up to about 90%.

3.3. Effect of tumour depth on the risk of secondary cancer

Under the PA irradiation geometry, when the tumour diameter is 2 cm, the effect of the brain tumour depth on the risk of secondary cancer in organs is explored. The depths of the brain tumour selected are 3, 4, 5 and 6 cm. For the 10- and 15-year-old female patients, the treatment times are 14.7, 17.5, 21.9, and 28.4 min and 14.3, 17.2, 21.8 and 27.8 min, respectively, for the tumours with various depths. The equivalent dose of the organs is shown in figure 8. As the depth of the tumour increases, the equivalent dose of the organs also increases.

The risks of secondary cancer in organs with different depths of tumours are shown in table 3. The overall LARs in the healthy organs of the 10-year-old female patients with various tumour depths are 369, 453, 622 and 809 per 100 000 population. The brain carries the highest LAR, with a 400 per 100 000 population lifetime risk of a secondary brain malignancy with a tumour depth of 6 cm at 10 years of age. In our calculations, brain tumours

Table 2. Lifetime attributable risks in organs and ages at exposure for different tumour diameters (per 100 000 population).

	Females (10 yr)			Females (15 yr)		
	1 cm (95% CI[a])	2 cm (95% CI)	5 cm (95% CI)	1 cm (95% CI)	2 cm (95% CI)	5 cm (95% CI)
Brain	290 (109, 568)	400 (150, 784)	457 (171, 895)	167 (63, 327)	214 (80, 419)	284 (106, 555)
Thyroid	96 (26, 358)	130 (35, 483)	183 (49, 681)	58 (15, 214)	74 (20, 275)	102 (27, 379)
Oesophagus	29 (<0, 116)	39 (<0, 157)	47 (<0, 186)	22 (<0, 87)	34 (<0, 136)	32 (<0, 128)
Right lung	76 (52, 111)	84 (57, 123)	120 (81, 174)	51 (34, 74)	57 (39, 83)	80 (54, 116)
Left lung	57 (39, 84)	64 (43, 93)	91 (61, 132)	35 (24, 51)	40 (27, 58)	56 (38, 81)
Breast	52 (37, 74)	58 (41, 81)	81 (58, 115)	44 (32, 63)	49 (35, 70)	69 (49, 97)
Liver	5 (2, 14)	6 (2, 17)	8 (3, 24)	3 (1, 8)	3 (1, 9)	4 (2, 13)
Stomach	11 (7, 17)	12 (8, 19)	17 (11, 26)	5 (3, 8)	7 (4, 10)	9 (6, 14)
Pancreas	3 (<0, 7)	4 (<0, 9)	5 (<0, 13)	1 (<0, 3)	2 (<0, 4)	3 (<0, 8)
Colon	3 (1, 6)	4 (2, 8)	5 (2, 11)	3 (1, 5)	3 (1, 7)	4 (2, 9)
Leukaemia	5 (1, 11)	6 (1, 14)	8 (1, 20)	3 (0, 8)	4 (0, 9)	5 (1, 16)
Bladder	1 (0, 2)	1 (0, 3)	1 (1, 3)	0 (0, 1)	1 (0, 1)	1 (0, 2)
Uterus	0 (<0, 0)	1 (<0, 1)	1 (<0, 3)	0 (<0, 0)	0 (<0, 1)	1 (<0, 2)

[a] CI represents the confidence intervals for LAR using the 95% range of β according to the BEIR VII report [17] and the study by Berrington de Gonzalez *et al* [18].

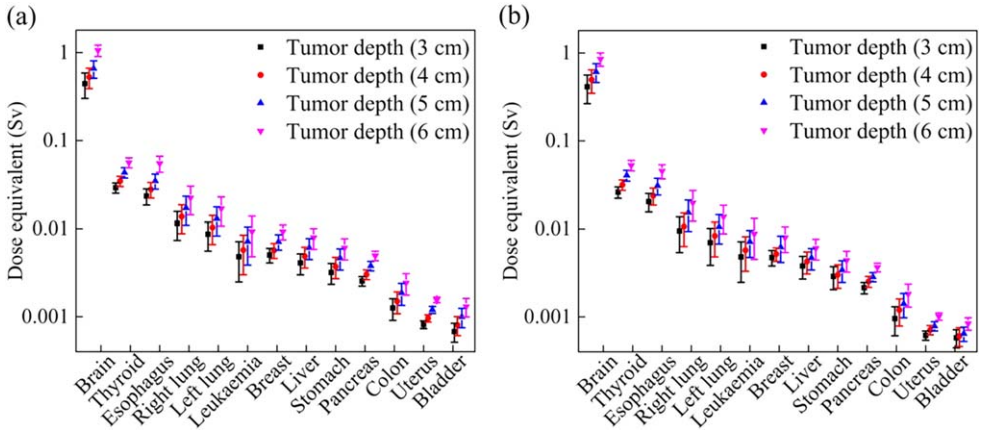

Figure 8. Organ equivalent dose for different tumour depths: (a) female patients aged 10 years, (b) female patients aged 15 years. (The error bar is the standard deviation.)

account for approximately 49.5% of all secondary cancers. As the depth of the tumour increases from 3–6 cm for the female patients aged 10 and 15 years old, the risk of secondary cancer in most organs increases more than twice, such as the thyroid, oesophagus, lung, breast, liver, etc.

3.4. Effect of gender and age on the risk of secondary cancer

Under the PA irradiation geometry, the 10- and 15-year-old male radiation computational phantoms are selected to study the effect of gender and age on the risk of secondary cancer. The brain tumour is the same as that of the female patients, with a diameter of 2 cm and a depth of 6 cm. The treatment times are 28.9 and 28 min for the 10- and 15-year-old male patients, respectively. The doses for the organs at risk do not exceed the limit, and the maximum doses of the skin are 11.55 and 11.37 Gy-Eq, respectively.

The equivalent dose of the organs is shown in figure 9. The organ equivalent dose of the male patients aged 10 and 15 are lower than these of the female patients of the same age. In organs that are far from the head, such as the stomach, pancreas, colon and bladder, the difference in equivalent dose is more obvious. Regarding the organ dose, the trend of male patients and female patients is the same. The farther away from the head, the equivalent dose of the healthy organs of concern also tends to decrease. As the patient ages from 10 to 15 years old, the equivalent doses for the organs are generally reduced, and the magnitude of the reduction in the organs' equivalent dose in male and female patients is similar.

The risks of secondary cancer in the organs of the 10- and 15-year-old male and female patients are shown in table 4. The risk of secondary cancer is greater in the organs of female patients than in those of male patients, especially in the thyroid, stomach and lung. But for the brain and oesophagus, the LAR in male patients is higher than that of female patients. This is because the baseline incidence of oesophageal cancer in males is much higher than that in females, and the β value in the LAR of the brain is much higher in males than in females according to the study by Berrington de Gonzalez *et al* [18]. For the male and female patients, as the age increases from 10 to 15 years, the risk of secondary cancer in the organs is reduced. For both male and female patients, the risks of secondary cancer are greater in the thyroid,

Table 3. Lifetime attributable risks in organs and ages at exposure with different tumour depths (per 100 000 population).

	Females (10 yr)				Females (15 yr)			
	3 cm (95% CI[a])	4 cm (95% CI)	5 cm (95% CI)	6 cm (95% CI)	3 cm (95% CI)	4 cm (95% CI)	5 cm (95% CI)	6 cm (95% CI)
Brain	182 (68, 357)	214 (80, 419)	302 (113, 591)	400 (150, 784)	103 (39, 202)	124 (47, 243)	152 (57, 297)	214 (80, 419)
Thyroid	64 (17, 238)	81 (22, 302)	105 (28, 389)	130 (35, 483)	35 (9, 129)	43 (11, 158)	58 (16, 216)	74 (20, 275)
Oesophagus	15 (<0, 61)	23 (<0, 92)	32 (<0, 127)	39 (<0, 157)	11 (<0, 43)	14 (<0, 57)	22 (<0, 86)	34 (<0, 136)
Right lung	38 (26, 56)	47 (32, 69)	66 (44, 96)	84 (57, 123)	26 (17, 38)	32 (21, 46)	53 (35, 77)	57 (39, 83)
Left lung	30 (20, 43)	38 (26, 55)	49 (33, 72)	64 (43, 93)	17 (12, 25)	23 (15, 33)	31 (21, 45)	40 (27, 58)
Breast	23 (17, 33)	30 (21, 42)	40 (29, 57)	58 (41, 81)	26 (18, 36)	30 (22, 43)	38 (27, 54)	49 (35, 70)
Liver	3 (1, 7)	3 (1, 9)	5 (2 13)	6 (2 17)	2 (1 5)	2 (1 6)	2 (1 7)	3 (1, 9)
Stomach	6 (4 9)	8 (5, 13)	11 (7 16)	12 (8, 19)	4 (3 6)	5 (3, 7)	6 (4 8)	7 (4, 10
Pancreas	2 (<0, 4)	2 (<0, 5)	3 (<0, 7)	4 (<0, 9)	1 (<0, 2)	1 (<0, 2)	1 (<0, 3)	2 (<0, 4)
Colon	2 (1 3)	2 (1, 5)	3 (1, 6)	4 (2 8)	1 (1 2)	1 (1 3)	2 (1 3)	3 (1, 7)
Leukaemia	3 (0, 6)	4 (0, 9)	5 (1 11)	6 (1 14)	2 (0, 4)	3 (0, 6)	3 (0, 7)	4 (0, 9)
Bladder	1 (0, 1)	1 (0, 1)	1 (0, 2)	1 (0, 3)	0 (0, 1)	0 (0, 1)	0 (0, 1)	1 (0, 1)
Uterus	0 (<0, 0)	0 (<0, 1)	0 (<0, 1)	1 (<0, 1)	0 (<0, 0)	0 (<0, 1)	0 (<0, 1)	0 (<0, 1)

[a] CI represents the confidence intervals for LAR using the 95% range of β according to the BEIR VII report [17] and the study by Berrington de Gonzalez *et al* [18].

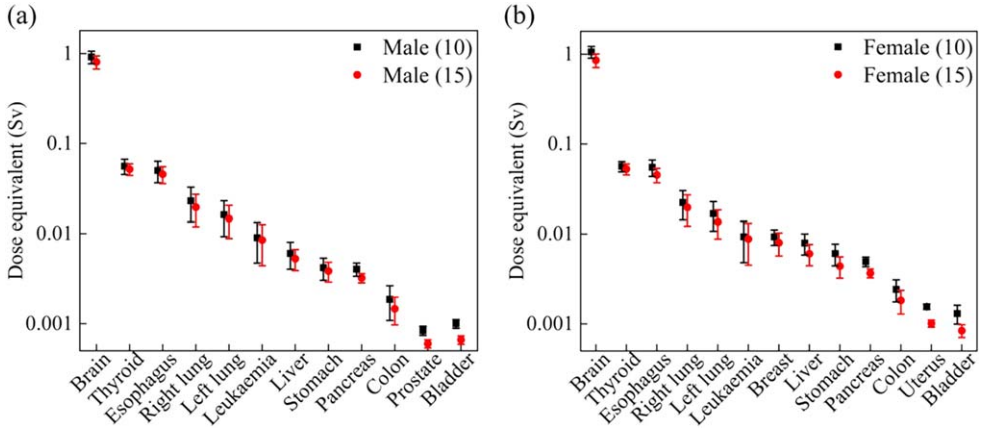

Figure 9. Organ equivalent dose: (a) 10- and 15-year-old male patients, (b) 10- and 15-year-old female patients. (The error bar is the standard deviation.)

Table 4. Lifetime attributable risks in organs and ages at exposure for different genders (per 100 000 population).

	Males (10 yr) (95% CI[a])	Males (15 yr) (95% CI)	Females (10 yr) (95% CI)	Females (15 yr) (95% CI)
Brain	983 (360, 1855)	539 (197, 1017)	400 (150, 784)	214 (80, 419)
Thyroid	22 (6, 82)	10 (3, 39)	130 (35, 483)	74 (20, 275)
Oesophagus	75 (<0, 170)	47 (<0, 108)	39 (<0, 157)	34 (<0, 136)
Right lung	48 (23, 104)	27 (13, 59)	84 (57, 123)	57 (39, 83)
Left lung	34 (16, 73)	20 (10, 44)	64 (43, 93)	40 (27, 58)
Liver	12 (6, 26)	7 (3, 14)	6 (2, 17)	3 (1, 9)
Stomach	9 (5, 17)	5 (3, 10)	12 (8, 19)	7 (4, 10)
Pancreas	4 (<0, 10)	2 (<0, 4)	4 (<0, 9)	2 (<0, 4)
Colon	6 (3, 10)	3 (2, 5)	4 (2, 8)	3 (1, 7)
Leukaemia	5 (0, 11)	3 (0, 7)	6 (1, 14)	4 (0, 9)
Bladder	1 (0, 3)	0 (0, 1)	1 (0, 3)	1 (0, 1)
Uterus/prostate	0 (<0, 1)	0 (<0, 0)	1 (<0, 1)	0 (<0, 1)
Breast	—	—	58 (41, 81)	49 (35, 70)

[a] CI represents the confidence intervals for the LAR using the 95% range of β according to the BEIR VII report [17] and the study of Berrington de Gonzalez *et al* [18].

lung and oesophagus than in the other organs. Especially, the LARs in the breast are high in the organs concerned for the 10- and 15-year-old female patients.

4. Discussion

The risks of secondary cancer in organs induced by BNCT in 10- and 15-year-old children with brain tumours are investigated in this study. Our study shows that the risks of secondary cancer in healthy organs depend significantly on the irradiation geometry in BNCT. In our

calculations, the overall organ LARs are 828, 1074 and 809 per 100 000 population for the three irradiation geometries (i.e., RLAT, TOP and PA) of the 10-year-old female patients. This result indicates that the PA geometry produces less scatter dose than the RLAT and TOP geometries, which translates into a lower risk of secondary cancer. The organ-specific LARs in the right lung, liver, pancreas, colon, uterus and bladder are much higher with the TOP irradiation geometry than with the two other geometries. This result suggests that radiation protection measures should be applied to the abdominal organs, especially the lungs, when the TOP irradiation geometry is used for BNCT.

Furthermore, the risk of secondary cancer increases with increasing tumour volume and depth. For example, when the tumour diameters of the 10-year-old female patients change from 1–5 cm, the risk of secondary cancer of the organs increases from 628–1024 per 100 000 population. When BNCT is applied to large tumours, adopting the multi-field irradiation strategy may reduce the risk of secondary cancer of the organs. Thus, this strategy merits being explored in future research. In our study, the risks of secondary cancer in females are larger than in males possibly because of the thinner body shielding thickness and the weaker protective effect on the internal organs of females than males. Most importantly, it is primarily because the parameter β of ERR and EAR in equation (1) is higher for female patients than for male patients in the calculation of LAR. The calculation results show that the risk of secondary cancer decreases with age at exposure. Paganetti *et al* [10] also showed that the risk of secondary cancer is significantly lower in the organs of 14-year-old patients than in those of 4-year-old patients receiving proton therapy. This finding could be related to the height and life expectancy of the patients. Thus, the risk of secondary cancer in the organs of BNCT-treated younger patients, especially the females, warrants careful consideration. With sufficient data, future studies may evaluate treatment plans of BNCT based not only on conventional factors from the dose volume histogram but also based on secondary cancer risk assessments.

The present study has some limitations. The irradiation room, bed, and instrument components are not considered in the simulation of BNCT. However, Hsiao *et al* [31] showed that the irradiation room and bed exert minimal effects on the organ dose. The tumours used in this study are regular-shaped spheroid tumours, which may be somewhat different from the realistic situation of tumours treated. However, this study can still serve as a reference for clinical treatment in BNCT.

5. Conclusion

The risks of secondary cancer for three irradiation geometries adopted in BNCT to treat brain tumours 2 cm in diameter and 6 cm in depth are assessed in this study. The results show that the risk of secondary cancer is lower with the PA irradiation geometry than with the RLAT and TOP irradiation geometries. Under the PA irradiation geometry, the LARs of organs significantly increase with tumour volume and depth. In addition, the risk of secondary cancer of the 10-year-old patients is higher than that of the 15-year-old patients and male patients have a lower risk of secondary cancer than female patients. From the perspective of secondary cancer, these findings provide some information about the risk of secondary cancer for the clinical application of BNCT.

Acknowledgements

This work was supported by the National Natural Science Foundation of China (Grant No. 11805100); the Natural Science Foundation of Jiangsu Province (Grant No. BK20180415); the National Key Research and Development Program (Grant Nos. 2016YFE0103600 and 2017YFC0107700); and the Foundation of Graduate Innovation Center in NUAA (Grant No. kfjj20180614).

ORCID iDs

Xiaobin Tang https://orcid.org/0000-0003-3308-0468

References

[1] Hopewell J W, Morris G M, Schwint A and Coderre J A 2011 The radiobiological principles of boron neutron capture therapy: a critical review *Appl. Radiat. Isot.* **69** 1756–9
[2] Kreiner A J, Bergueiro J, Cartelli D, Baldo M, Castell W, Asoia J G, Padulo J, Sandín J C S, Igarzabal M and Erhardt J 2016 Present status of accelerator-based BNCT *Rep. Pract. Oncol. Radiother.* **21** 95–101
[3] Kato I, Ono K, Sakurai Y, Ohmae M, Maruhashi A, Imahori Y, Kirihata M, Nakazawa M and Yura Y 2004 Effectiveness of BNCT for recurrent head and neck malignancies *Appl. Radiat. Isot.* **61** 1069–73
[4] Kreiner A J 2014 Accelerator-based BNCT *Appl. Radiat. Isot.* **88** 185–9
[5] Kumada H, Matsumura A, Sakurai H, Sakae T, Yoshioka M, Kobayashi H, Matsumoto H, Kiyanagi Y, Shibata T and Nakashima H 2014 Project for the development of the LINAC based NCT facility in University of Tsukuba *Appl. Radiat. Isot.* **88** 211–5
[6] Burian J, Flibor S, Marek M, Rejchrt J, Viererbl L and Tomandl I 2006 Physics for BNCT *J. Phys. Conf. Ser.* **41** 174
[7] Xu X G, Bednarz B and Paganetti H 2008 A review of dosimetry studies on external-beam radiation treatment with respect to second cancer induction *Phys. Med. Biol.* **53** R193
[8] Hoekstra N, Fleury E, Lara T R M, van der Baan P, Bahnerth A, Struik G, Hoogeman M and Pignol J-P 2018 Long-term risks of secondary cancer for various whole and partial breast irradiation techniques *Radiother. Oncol.* **128** 428–33
[9] Geng C, Moteabbed M, Xie Y, Schuemann J, Yock T and Paganetti H 2015 Assessing the radiation-induced second cancer risk in proton therapy for pediatric brain tumors: the impact of employing a patient-specific aperture in pencil beam scanning *Phys. Med. Biol.* **61** 12
[10] Wink K C J, Roelofs E, Simone C B II, Dechambre D, Santiago A, van der Stoep J, Dries W, Smits J, Avery S and Ammazzalorso F 2018 Photons, protons or carbon ions for stage I non-small cell lung cancer–results of the multicentric ROCOCO *in silico* study *Radiother. Oncol.* **128** 139–46
[11] Newhauser W D and Marco D 2011 Assessing the risk of second malignancies after modern radiotherapy *Nat. Rev. Cancer* **11** 438–48
[12] Nakagawa Y, Kageji T, Mizobuchi Y, Kumada H and Nakagawa Y 2009 Clinical results of BNCT for malignant brain tumors in children *Appl. Radiat. Isot.* **67** S27–30
[13] Geng C, Tang X, Hou X, Shu D and Chen D 2014 Development of Chinese hybrid radiation adult phantoms and their application to external dosimetry *Sci. China Technol. Sci.* **57** 713–9
[14] Tanaka K, Sakurai Y, Kajimoto T, Tanaka H, Takata T and Endo S 2016 Design study of multi-imaging plate system for BNCT irradiation field at Kyoto university reactor *Appl. Radiat. Isot.* **115** 212–20
[15] Sakurai Y, Tanaka H, Takata T, Fujimoto N, Suzuki M, Masunaga S, Kinashi Y, Kondo N, Narabayashi M and Nakagawa Y 2015 Advances in boron neutron capture therapy (BNCT) at Kyoto University—from reactor-based BNCT to accelerator-based BNCT *J. Korean Phys. Soc.* **67** 76–81

[16] Miyakawa A, Shibamoto Y, Takemoto S, Serizawa T, Otsuka S and Hirai T 2017 Fractionated stereotactic radiotherapy for metastatic brain tumors that recurred after gamma knife radiosurgery results in acceptable toxicity and favorable local control *Int. J. Clin. Oncol.* **22** 1–7
[17] National Research Council 2006 *Health Risks from Exposure to Low Levels of Ionizing Radiation BEIR VII Phase 2* (Washington, DC: The National Academies Press)
[18] Berrington de Gonzalez A B, Apostoaei A I, Veiga L H S, Rajaraman P, Thomas B A, Hoffman F O, Gilbert E and Land C 2012 RadRAT: a radiation risk assessment tool for lifetime cancer risk projection *J. Radiol. Prot.* **32** 205
[19] Donovan E M, James H, Bonora M, Yarnold J R and Evans P M 2012 Second cancer incidence risk estimates using BEIR VII models for standard and complex external beam radiotherapy for early breast cancer *Med. Phys.* **39** 5814–24
[20] Perl J, Shin J, Schümann J, Faddegon B and Paganetti H 2012 TOPAS: an innovative proton Monte Carlo platform for research and clinical applications *Med. Phys.* **39** 6818–37
[21] Geng C, Tang X, Guan F, Johns J, Vasudevan L, Gong C, Shu D and Chen D 2015 GEANT4 calculations of neutron dose in radiation protection using a homogeneous phantom and a Chinese hybrid male phantom *Radiat. Prot. Dosimetry* **168** 433–40
[22] Wittig A, Michel J, Moss R L, Stecher-Rasmussen F, Arlinghaus H F, Bendel P, Mauri P L, Altieri S, Hilger R and Salvadori P A 2008 Boron analysis and boron imaging in biological materials for boron neutron capture therapy (BNCT) *Crit. Rev. Oncol. Hematol.* **68** 66–90
[23] Henriksson R, Capala J, Michanek A, Lindahl S-Å, Salford L G, Franzén L, Blomquist E, Westlin J-E and Bergenheim A T 2008 Boron neutron capture therapy (BNCT) for glioblastoma multiforme: a phase II study evaluating a prolonged high-dose of boronophenylalanine (BPA) *Radiother. Oncol.* **88** 183–91
[24] Shimosegawa E, Isohashi K, Naka S, Horitsugi G and Hatazawa J 2016 Assessment of 10 B concentration in boron neutron capture therapy: potential of image-guided therapy using 18 FBPA PET *Ann. Nucl. Med.* **30** 749–55
[25] Watabe T, Hanaoka K, Naka S, Kanai Y, Ikeda H, Aoki M, Shimosegawa E, Kirihata M and Hatazawa J 2017 Practical calculation method to estimate the absolute boron concentration in tissues using 18 F-FBPA PET *Ann. Nucl. Med.* **31** 481–5
[26] Liu Z and Chen J 2008 New calculations of neutron kerma coefficients and dose equivalent *J. Radiol. Prot.* **28** 185
[27] Edwards A A 1999 Neutron RBE values and their relationship to judgements in radiological protection *J. Radiol. Prot.* **19** 93
[28] Jingli Liu K, Kiger W S, Riley K J, Binns P J, Hemant P, Hopewell J W, Harling O K, Busse P M and Coderre J A 2008 Functional and histological changes in rat lung after boron neutron capture therapy *Radiat. Res.* **170** 60–9
[29] Coderre J A and Morris G M 1999 The radiation biology of boron neutron capture therapy *Radiat. Res.* **151** 1–18
[30] Coccia P F, Altman J and Bhatia S 2012 Adolescent and young adult oncology *J. Natl. Compr. Cancer Network* **10** 1112–50
[31] Hsiao M-C, Liu Y-H and Jiang S-H 2014 Computational study of room scattering influence in the THOR BNCT treatment room *Appl. Radiat. Isot.* **88** 162–6